Ophthal. Physiol. Opt. 2006 **26:** 264–280

Target detection and driving behaviour measurements in a driving simulator at mesopic light levels

Johan W. A. M. Alferdinck

TNO Human Factors, PO Box 23, Soesterberg, The Netherlands

Abstract

During night-time driving hazardous objects often appear at mesopic light levels, which are typically measured using light meters with a spectral sensitivity that is only valid for photopic light levels. In order to develop suitable mesopic models a target detection experiment was performed in a driving simulator. While subjects drove along a winding road they had to respond to randomly presented circular targets at various eccentricities. The background luminance ranged between 0.01 and 10 cd m^{-2}, and was either white, yellow, red or blue. The RT, number of missed targets, and driving behaviour were measured. The results show that target detection and driving performance get poorer with decreasing background luminance and increasing eccentricity of the target, in particular for the red colour. At high driving speeds and low luminances subjects tend to neglect left off-axis targets. Luminance calculated with existing reaction-time-based mesopic models fits better to RT data than the widely-used photopic luminance.

Keywords: driving behaviour, driving simulator, mesopic vision, RT, traffic

Introduction

General

Driving on the road at night-time is more risky than driving during the day. Only 25% of all traffic is present during the hours of darkness, but the number of accidents is roughly equal for night and day (Rumar, 2002). This justifies putting effort into research on perception in night-time road traffic in order to improve traffic safety after dark. One of the means to enhance traffic safety is improvement of automotive and street lighting. An adequate light level on the road will lead to higher visibility of objects, critical for the driving task, and will therefore result in lower accident rates. There is consensus that a higher level of street lighting results in a lower accident rate (De Clercq, 1985; Owens and Sivak, 1993; Vis, 1994).

The levels of street lighting normally differ by road type, traffic density, etc. (Kaptein *et al.*, 1997). The luminance levels of well-illuminated roads range from 1 to 2 cd m^{-2}. Rural roads with low traffic density in general have luminances between 0.1 and 1 cd m^{-2}. As the areas beside the road are normally not addressed by lighting recommendations, the luminance levels can be very low. However these areas are important for the detection of potential hazards, such as animals or pedestrians (Rea, 2001).

There is discussion in the lighting literature on the appropriateness of the spectral sensitivity of the light sensors that are used for measuring the light levels in the traffic scene, such as lux meters and luminance meters (Lewis, 1998; Lewis, 1999; Lewin, 2001; Rea, 2001). Currently, the standard spectral sensitivity established by the Commission Internationale de l'Eclairage/International Commission on Illumination (CIE), the spectral luminous efficiency function for photopic vision, $V(\lambda)$, (*Figure 1*) is widely used for light measuring equipment (CIE, 1986). However, this function, with a maximum sensitivity at 555 nm, is only valid for the photopic region with relatively high luminance levels of more than about

Received: 2 February 2005
Revised form: 21 April 2005
Accepted: 3 May 2005

Correspondence and reprints requests to: Johan W. A. M. Alferdinck.
Tel: +31 346 356 311; Fax: +31 346 353977.
E-mail address: johan.alferdinck@tno.nl

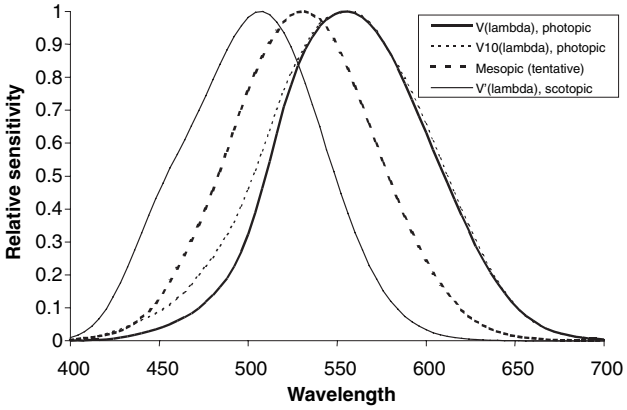

Figure 1. The CIE spectral luminous efficiency functions for photopic vision, $V(\lambda)$ and $V_{10}(\lambda)$, and scotopic vision $V'(\lambda)$ compared with an example of a tentative spectral mesopic function for a typical mesopic light level.

3 cd m^{-2} (CIE, 1978). Photopic vision is mainly determined by the cone receptors in the central part of the retina (fovea). The $V(\lambda)$ function is based on psychophysical measurements with a 2 degrees central test field. An alternative spectral luminous efficiency function, the $V_{10}(\lambda)$, is sometimes used for large stimuli, but it is not common for light meters (CIE, 1986). This spectral luminous efficiency function is based on psychophysical measurements with a 10 degree test field and has higher sensitivity in the blue part of the spectrum between 450 nm and 500 nm (*Figure 1*). When the light level decreases to luminances lower than about 1 cd m^{-2} the spectral sensitivity of the human eye shifts toward the blue and does not match with the $V(\lambda)$ or $V_{10}(\lambda)$ function. At luminances lower than 0.001 cd m^{-2} the visual perception is mainly determined by the rod receptors in the peripheral part of the retina. This is called scotopic vision. For this region the CIE has established the standard spectral luminous efficiency function for scotopic vision, $V'(\lambda)$, which has a maximum sensitivity at approximately 507 nm (*Figure 1*; CIE, 1983). The luminance range in between photopic and scotopic, from about 0.001 to 3 cd m^{-2}, is known as the mesopic domain (Wyszecki and Stiles, 1982). The location of the maximum along the wavelength axis and the shape of the mesopic spectral sensitivity function in this domain depend on the light level. A lower light level corresponds to a maximum sensitivity at a lower wavelength. *Figure 1* shows a tentative mesopic spectral sensitivity for a luminance somewhere in the middle of the mesopic range.

As part of the perception tasks in traffic, especially in the periphery of the visual field, have to be performed at mesopic light levels it is obvious that an appropriate spectral sensitivity must be incorporated in the light meters for these intermediate light levels. However, in spite of many proposals for spectral sensitivity functions in the mesopic domain, there is still no uniform standard recognised.

Mesopic models

In the past many attempts were made to develop a model for mesopic vision. Several authors have measured the spectral sensitivity functions in the mesopic domain (Walters and Wright, 1943; Kinney, 1958; Palmer, 1968; Kokoschka and Bodmann, 1975; Ikeda and Shimozono, 1981; Yaguchi and Ikeda, 1984; Sagawa and Takeichi, 1986; Sagawa and Takeichi, 1987; He *et al*., 1998). All these studies proposed a specific spectral sensitivity as a function of the adaptation light level in the mesopic range. However, it appeared to be difficult to establish a consistent mesopic model. In 1989 the CIE published a report on the status of mesopic photometry, without actually establishing a standard model for mesopic vision (CIE, 1989). After that publication new methods and refinements of the existing models were proposed. In 2001 a new CIE report was published (CIE, 2001), updating the CIE publication of 1989. Seven mesopic models were addressed in this publication, which are based on a 10 degrees visual field and heterochromatic brightness matching (HCBM). *Table 1* lists these mesopic models and their most important parameters, together with four mesopic models based on reaction time (RT) which were published elsewhere. With these models it is possible to calculate the so-called *equivalent luminance*, using various types of input variables. The equivalent luminance is defined as the luminance of the reference stimulus (formally with a wavelength of nearly 555 nm, but also often a broadband white light) that appears equal to the test stimulus in brightness (CIE, 2001). The equivalent luminance has a better correlation to the visual impression or task performance than the common photopic luminance based on the $V(\lambda)$ function. Instead of the more formal term equivalent luminance, the term *mesopic luminance* will be used in this study to designate the output of mesopic models.

The seven models are based on HCBM experiments in which the task of the subjects was to match the brightness of two parts of a static stimulus with a diameter of 10 degrees. The currently widely-used luminous efficiency function for photopic vision, $V(\lambda)$, is mainly based on flicker photometry using a 2 degree field in which the two parts of the stimulus are compared by presenting them in an alternating mode. These differences in the tasks and conditions result in different shapes of the spectral sensitivity function in photopic conditions. A stimulus with a saturated colour (e.g. monochromatic blue or red) that has the same luminance as a white stimulus is perceived as brighter than the white stimulus. This effect is known as the Helmholtz–Kohlrausch effect (Wyszecki and Stiles, 1982). Therefore the spectral sensitivity functions based on photopic brightness matching are wider than the luminous efficiency function $V(\lambda)$ which is incorporated in the

Table 1. Mesopic models in the 2001 CIE report (No. 1–7) and the models of He and Rea (No. 8–11)

No.	Model	Field diameter (degrees)	Task	Eccentricity (degrees)	Input variables	References
1	Palmer 1	10	HCBM	0	L_{10}, L'	Palmer, 1968
2	Palmer 2	10	HCBM	0	L_{10}, L'	CIE, 1989, 2001
3	Sagawa-Takeichi	10	HCBM	0	L_{10}, L', X, Y, Z	Ikeda and Shimozono, 1981; CIE, 1989
4	Nakano-Ikeda	10	HCBM	0	L', X_{10}, Y_{10}, Z_{10}	Sagawa and Takeichi, 1987, 1992
5	Kokoschka-Bodmann	10	HCBM	0	L', X_{10}, Y_{10}, Z_{10}	Kokoschka and Bodmann, 1975; Kokoschka, 1980
6	Trezona	10	HCBM	0	L', X_{10}, Y_{10}, Z_{10}	Trezona, 1987, 1990
7	Ashizawa	10	HCBM	0	$V_{10}(\lambda)$, $V'(\lambda)$	Ashizawa *et al.*, 1985
8	He 1	2	RT	15	$L_e(\lambda)$	He *et al.*, 1997
9	He 2	2	RT	12	$L_e(\lambda)$	He *et al.*, 1998
10	Rea	2	RT	Non-foveal	$L_e(\lambda)$	Rea *et al.*, 2003
11	UnifL	2	RT	Non-foveal	L, L'	Rea *et al.*, 2004

HCBM, heterochromatic brightness matching; X, Y, Z, tristimulus values according to the CIE 1931 standard colorimetric system (2 degree field size) (CIE, 1986); X_{10}, Y_{10}, Z_{10}, tristimulus values according to the CIE 1964 supplementary standard colorimetric system (10 degree field size); $V(\lambda)$, spectral luminous efficiency function for photopic vision (2 degrees field size) (CIE, 1986); $V_{10}(\lambda)$, spectral luminous efficiency function for photopic vision (10 degrees field size); $V'(\lambda)$, spectral luminous efficiency function for scotopic vision; L, photopic luminance based on $V(\lambda)$; L_{10} ($=Y_{10}$), photopic luminance based on $V_{10}(\lambda)$; L', scotopic luminance based on $V'(\lambda)$; $L_e(\lambda)$, spectral radiance.

vast majority of all luminance meters and illuminance meters. The spectral luminous efficiency function for scotopic vision, $V'(\lambda)$, is determined by HCBM using a 20 degree field (CIE, 1983).

Thus, because of differences in task and stimulus diameter, it is difficult to merge the sensitivity functions to a single model. There is no smooth connection between the existing spectral sensitivity data in the mesopic domain and the current spectral sensitivity standards for scotopic, $V'(\lambda)$, at the lower end of the mesopic range, and for photopic vision, $V(\lambda)$, at the higher end of the mesopic range. The problem of the difference in the field size can be solved by applying the spectral luminous efficiency function for the 10 degree CIE-observer, $V_{10}(\lambda)$, for the photopic domain, instead of the more generally used spectral luminous efficiency function for the 2-degree CIE-observer, $V(\lambda)$.

Another problem is that the spectral sensitivity functions based on brightness matching suffer from a failure of additivity. Additivity is essential for photometry (Abney's law). The additivity problem can be tackled by using flicker photometry or a similar method. The $V(\lambda)$ and $V_{10}(\lambda)$ functions are based on flicker photometry and have been shown to obey Abney's law (Wyszecki and Stiles, 1982). The models 8 and 9 in *Table 1* are based on RT. The authors claim that these models do not suffer from the problems of models which are based on brightness matching (He *et al.*, 1997, 1998). They state that in a RT task, just as in flicker photometry, the fast magnocellular channel, rather than the slow parvocellular channel, is being used. It is thought that the magnocellular channel is used for the fast transportation of the brightness signal; the parvocellular channel is slower and transports both the brightness and colour signals. Only the magnocellular channel appears to obey Abney's law of additivity. Therefore the results of the RT experiments can be directly compared with luminance data obtained with the spectral luminous efficiency functions for photopic vision, $V(\lambda)$ and $V_{10}(\lambda)$. As both He models include peripheral measurements these models make use of the wide field $V_{10}(\lambda)$ rather than the $V(\lambda)$ for describing the luminance at photopic light levels. Foveal vision measured by RTs might be modelled by $V(\lambda)$ for any light level (He *et al.*, 1997).

The RT task is directly linked to the performance task of driving a vehicle. One of the tasks of driving a vehicle is avoiding a potential hazard on the road and therefore a fast reaction is essential. Potential hazards, such as cars, pedestrians, and animals, do not always appear in front of the car, often they can come into view from the side. For that reason off-axis detection is also important. The rods play an important role for off-axis detection, so the photopic luminance based on the $V(\lambda)$ function is inadequate. It should be noted that the first seven models in *Table 1* do not account for the eccentricity of the stimulus, i.e. eccentricity is not a parameter in the model.

Models 8, 9, 10, and 11 are all based on RT measurements of two studies (He *et al.*, 1997, 1998). Model 8 is based on the calculation of the spectral luminous efficiency function for mesopic vision, $V_{mes}(\lambda)$, by weighting the spectral luminous efficiency function for scotopic vision, $V'(\lambda)$, and the spectral luminous efficiency function for photopic vision with 10 degrees field size, $V_{10}(\lambda)$ according to equation:

$$V_{mes}(\lambda, L_{mes}) = k\{x(L_{mes})V_{10}(\lambda) + [1 - x(L_{mes})]V'(\lambda)\}. \quad (1)$$

The weighting factor, x, depends on the light level. The factor k is a normalisation constant which ensures

that the maximum value of $V_{mes}(\lambda)$ is unity. The mesopic luminance, L_{mes}, is calculated by applying the calculated spectral luminous efficiency function for mesopic vision in the integration over the visual part of the spectrum according to equation:

$$L_{mes} = K_{mes} \int V_{mes}(\lambda, L_{mes}) L_e(\lambda) d\lambda. \quad (2)$$

The factor K_{mes} is equal to 683 lm W^{-1} divided by the value of $V_{mes}(\lambda)$ for a wavelength of $\lambda = 555$ nm and $L_e(\lambda)$ is the spectral radiance in $W\ m^{-2}\ s^{-1}$. Note that the light level used to calculate the weighting factor x in turn is used as mesopic luminance. Hence, the calculation of the mesopic luminance is a complicated iterative algorithm that must be repeated until a sufficiently accurate value of L_{mes} is obtained.

Model 9 differs from model 8 because of a slightly different function for the weighting factor. The algorithm is also iterative and more complicated because the light level is expressed as mesopic retinal illuminance (in trolands) rather than as mesopic luminance. Model 9 also determines the spectral luminous efficiency function for mesopic vision, $V_{mes}(\lambda)$, by weighting the spectral luminous efficiency functions $V'(\lambda)$ and $V_{10}(\lambda)$.

Model 10 is designed according to the same weighting principle as applied in models 8 and 9. The difference is that now the more common efficiency function for photopic vision for a 2 degree field size, $V(\lambda)$, is used instead of $V_{10}(\lambda)$. The second simplification is that the weighting factor is a function of the photopic luminance L and the ratio of scotopic and photopic luminance, S/P (2 degree observer). Therefore the calculation procedure is not iterative.

Model 11, the unified luminance model, is the simplest model (Rea *et al*., 2004), which only needs the *photopic luminance* and *scotopic luminance* as input, rather than the spectral radiance data as in previous models. The model consists of a closed form equation and the calculation is not iterative.

As the RT task is highly relevant for traffic, and additivity is preserved, it can be concluded that spectral sensitivity determined with a RT task would seem to be a promising candidate for a mesopic model.

Mesopic experiments in a driving context

Three previous studies of target detection at mesopic light levels in a driving context were identified (*Table 2*). Two experiments were conducted in the laboratory and one was a field experiment in a real car. In all experiments the target was presented in the periphery of the visual field. The target size ranged from 1 to 3 degrees and the target eccentricities varied between 12 and 29 degrees. The luminance of the background was in the mesopic range between 0.1 and 3 cd m^{-2}. The last column in *Table 2* gives an indication of the colour of the stimulus. The S/P ratio is the ratio between the scotopic and photopic (2 degree observer) luminance. This ratio is high when the colour is bluish and low when the colour is yellowish or reddish.

In the first laboratory experiment the driving task was simulated with a commercial racing game (Bullough and Rea, 2000). The scene was projected on a screen. The subjects were able to control the 'car' with a steering wheel and an accelerator pedal and were asked to drive as quickly and safely as possible. The luminance level and the colour of the scene (S/P ratio) were controlled by neutral density filters mounted in front of the projector lens. During the runs the target was presented for about half a second at random time intervals. Subjects were asked to respond verbally. It appeared that with increasing background luminance the driving speed increased and the number of crashes decreased. There was no effect of colour on speed and number of crashes. Subjective brightness rating increased with luminance, with no effect of colour. The detection of targets improved for higher background luminances (less missed targets). The percentage of missed targets decreased with increasing S/P ratio, i.e. more bluish colour. This effect of colour was seen for all background luminances between 0.1 and 3 cd m^{-2}. This means that a more bluish light colour helps with

Table 2. Parameters of target detection experiments in a driving context

Experiment	Target size (degrees)	Target eccentricity (degrees)	Target contrast $[(L_t - L_b)/L_b]$	Background luminance, photopic (cd m^{-2})	S/P
Laboratory (Bullough and Rea, 2000)	2.4 × 3	18	0.78	0.1, 0.3, 1, 3	0.64 (HPS) 1.35 (Red) 1.78 (MH) 3.77 (Blue)
Laboratory (Lingard and Rea, 2002)	2 (circular)	12, 18, 24, 29	0.1, 0.4, 0.7, 1.0	0.1, 0.3, 1, 3	0.5 (HPS) 1.8 (MH)
Field experiment (Akashi and Rea, 2002)	1.38 × 0.94 1.32 × 0.89	15, 23	2.77	0.19	0.6 (HPS) 1.5 (MH)

S/P, ratio between scotopic and photopic luminance (2 degree observer); HPS, high-pressure sodium lamp; MH, metal halide lamp.

object detection in the periphery, even at photopic light levels.

In the second laboratory study (Lingard and Rea, 2002), subjects were required to negotiate a projected computer-generated roadway course while responding to targets in the periphery. The subjects controlled direction and speed by using the arrow keys of a computer keyboard with their right hand. The left hand was used to activate a switch when a target was detected. Filters in front of the projector controlled the light level and the colour. The RT and detection rate (percentage correct) was measured. The RT decreased and the detection rate increased with increasing background luminance and target contrast. For a low background luminance, particularly for low contrasts, the off-axis RT was smaller and the detection rate was higher for the metal halide (MH) lamp (large S/P ratio) than for the high pressure sodium (HPS) lamp (low S/P ratio).

In the field experiment (Akashi and Rea, 2002) the subjects drove in a car along a track at a parking lot. The targets of different contrast and eccentricity appeared at the side of the road. The scene was illuminated with HPS or MH lamps at an equal light level (photopic illuminance of about 5.5 lux). The RTs and missed targets were measured. The RTs for an eccentricity of 15 degrees were shorter than for 23 degrees. The RTs under MH illumination were lower than under HPS illumination. Moreover, there was a significant interaction between eccentricity and lamp type; the difference between HPS and MH was most pronounced for the largest eccentricity of 23 degrees.

These three experiments clearly show that photopic photometry does not adequately describe the performance of peripheral target detection at mesopic light levels. In a simulated driving task using low background luminances and low contrasts, RTs are shorter and the number of missed targets are lower when the bluish light (large S/P ratio) is applied instead of yellowish light (low S/P ratio). In other words, for an equal detection performance in the periphery the photopic light level of yellow objects must be higher than that of blue objects.

MOVE project

In order to develop a standard method for measuring light in the mesopic domain, or at least try to make a firm step forward in drafting a practical model for mesopic vision, the European project 'Mesopic Optimisation of Visual Efficiency' (MOVE) was started. The main goal of the project is to perform visual research in order to establish a standard spectral efficiency function for mesopic vision (Eloholma and Halonen, 2003). The establishment of an internationally-accepted standard for mesopic vision is considered to be very important for the design of street lighting. Therefore the MOVE project is mainly focussed on the benefits of street lighting for road traffic. The project partners have carried out experiments on perception at mesopic light levels in the laboratory and in field experiments (Eloholma *et al*., 2005). The results will be collected and used to develop a mesopic model.

Within the framework of the MOVE project we performed perception and driving behaviour experiments in our driving simulator at mesopic light levels. Subjects drove a simulated winding road while targets were presented at random eccentricities. The RT, missed targets and driving behaviour were measured. This paper describes the main RT experiment in the driving simulator. The results were then used to test existing mesopic models based on RT.

Methods

Apparatus

The target detection experiment was performed in the high-fidelity TNO driving simulator (*Figure 2*). The simulator has a real car body and real dashboard instruments. The distance between the driver's eyes and curved projection screen is 3.75 m. The road scene is 120 degrees wide and projected with three projectors, each 40 degrees wide and 30 degrees high, corresponding to an image height of 2.1 m and an image width (along the arc) of 2.6 m. The resolution of each projector is 1280×1024 pixels. The maximum image luminance (white) is about 25 cd m^{-2}. The colour of the light was controlled by setting the RGB values of the driving simulator imaging system. Four colours were used in the experiment, white, yellow, red, and blue. In order to match the luminances of these colours to the

Figure 2. TNO driving simulator consisting of a fully equipped car body on a moving base and a 120×30 degree projection screen.

desired luminances the RGB values (maximum: 1,1,1) of the colour were set to (0.88, 0.88, 0.88), (1,1,0), (0.9,0,0), and (0,0,0.8) for white, yellow, red, and blue, respectively.

The subjects wore goggles during the experiment. The overall luminance level was controlled by putting the appropriate neutral density filters in these goggles. Three neutral filters were used with densities of 1, 2, and 3 (density $D = -\log_{10}(T)$ where T is the transmission: nominal transmissions in the photopic region of 0.1, 0.01 and 0.001). In the case when no neutral density filters were needed the goggles were worn without a filter (density 0, transmission 1). The spectral transmissions of the filters and the windscreen are shown in *Figure 3*. The viewing angle of the goggles was large enough to cover the target eccentricities. The field of view through the windscreen was limited by the left wind screen post at about −30 degrees and by the right windscreen post at about +60 degrees.

The spectral radiance of the background was measured for all four colours. The background is defined as the area surrounding the target, the roadside below the horizon (*Figure 5*). In a separate experiment on a computer monitor, not further described here, it was shown that there was no difference in performance between the road scene background of *Figure 5* and a uniform background with the same luminance as the roadside.

Figure 4 shows spectral radiance of the background averaged over eccentricities between −15 and +15 degrees, without taking into account the transmission of the windscreen and the neutral filters in the goggles. *Table 3* presents the desired luminance, colours, density of filter applied, and the actual luminance obtained according to various photopic, scotopic and mesopic models. The actual luminances are determined while taking into account that the spectral transmissions of the goggles and the windscreen are averaged over the eccentricities between −15 and +15 degrees. The obtained luminances are somewhat higher than the desired luminances. It was not possible to create red and blue backgrounds with a luminance of 10 cd m^{-2}. Note also that the S/P ratio (scotopic luminance divided by photopic 2 degree luminance) is listed. The average S/P ratios for white, yellow, red, and blue are 2.12, 1.39, 0.22, and 9.08.

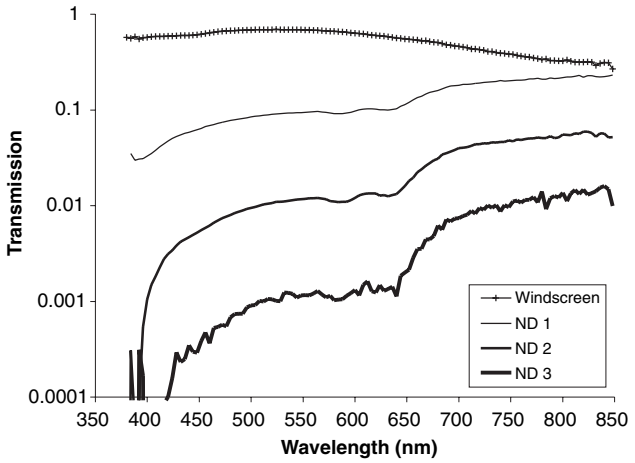

Figure 3. Transmission of the windscreen and the neutral density (ND) filters in the goggles.

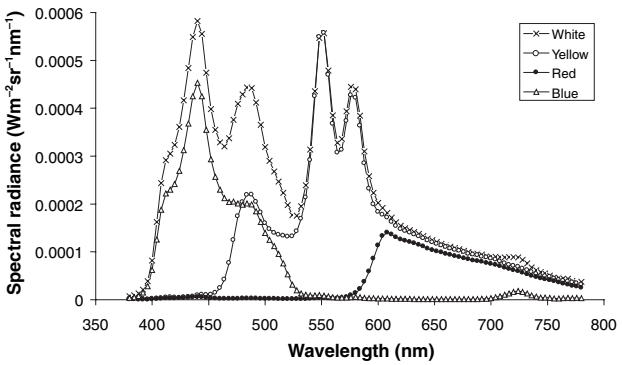

Figure 4. Spectral radiance of the background, averaged over eccentricities between −15 degrees and +15 degrees, without windscreen or neutral density filters.

Traffic scene and target

The modelled traffic scene was kept very simple. *Figure 5* shows the middle part of the projection (40 degrees wide). The target could appear at eccentricities of −15, −10, −5, +5, +10, +15 degrees. The eccentricities were defined with reference to the heading direction of the car. As in a real driving task, the subjects could freely move their eyes to fixate at any point in the scene.

The circular target subtended a visual angle of 2 degrees. The centre of the target was always 1.1 degree below the horizon. (In the simulation modelling program a circular object was modelled with a diameter of 1.215 m, located on the ground, at 35 m in front of the driver's eye). The average contrast of the target [$C = (L_t - L_b)/L_b$, with L_t = target luminance and L_b = background luminance) was 0.14 with a standard deviation of 0.06.

The subject had to drive on a one-lane road with some curves. The width of the road between the lines was 3.5 m. The line width was 10 cm. The length of the route driven was about 6 km. The eye of the driver was modelled at 1.28 m above the ground. In order to be sure of the appropriate luminance, colour, and contrast the area adjacent to the road scene was designed with simple graphics and minimal structure. As there were no buildings, trees or road structures adding, texture is

Table 3. The desired luminance for the various conditions compared with the obtained average background luminances calculated with CIE photopic 2 degrees, photopic 10 degrees, scotopic, and four mesopic spectral efficiency functions (See *Table 2*)

		Luminance (cd m^{-2})								
		Desired	Obtained				Mesopic luminance (cd m^{-2})			
Colour	Neutral density filter	Photopic, 2 degrees	Photopic, 2 degrees	Photopic, 10 degrees	Scotopic	S/P	He 1	He 2	Rea	UnifL
White	0	10	13.5	14.8	33.7	2.50	14.8	14.8	13.5	13.5
Yellow	0	10	11.3	11.8	17.1	1.51	11.8	11.8	11.3	11.3
Red	–	10	–	–	–	–				
Blue	–	10	–	–	–	–				
White	1	1	1.25	1.35	2.74	2.19	1.35	1.35	1.25	1.25
Yellow	1	1	1.06	1.11	1.51	1.42	1.11	1.11	1.06	1.06
Red	0	1	1.16	1.21	0.287	0.247	1.21	1.21	1.16	1.16
Blue	0	1	1.30	1.96	13.1	10.1	1.96	1.96	1.30	1.30
White	2	0.1	0.152	0.163	0.301	1.980	0.219	0.216	0.213	0.215
Yellow	2	0.1	0.131	0.135	0.177	1.353	0.158	0.157	0.155	0.156
Red	1	0.1	0.117	0.122	0.0247	0.211	0.0511	0.0587	0.0522	0.0386
Blue	1	0.1	0.108	0.156	0.967	8.99	0.359	0.338	0.285	0.327
White	3	0.01	0.0151	0.0160	0.0273	1.81	0.0265	0.0254	0.0253	0.0262
Yellow	3	0.01	0.0131	0.0135	0.0169	1.30	0.0172	0.0168	0.0168	0.0168
Red	2	0.01	0.0151	0.0157	0.0028	0.188	0.00324	0.00391	0.00379	0.00305
Blue	2	0.01	0.0120	0.0168	0.0975	8.15	0.0726	0.0657	0.0639	0.0755

S/P, scotopic/photopic ratio. The luminances are averaged over the eccentricities between −15 and +15 degrees and are determined while taking into account the spectral transmissions of the goggles and the windscreen.

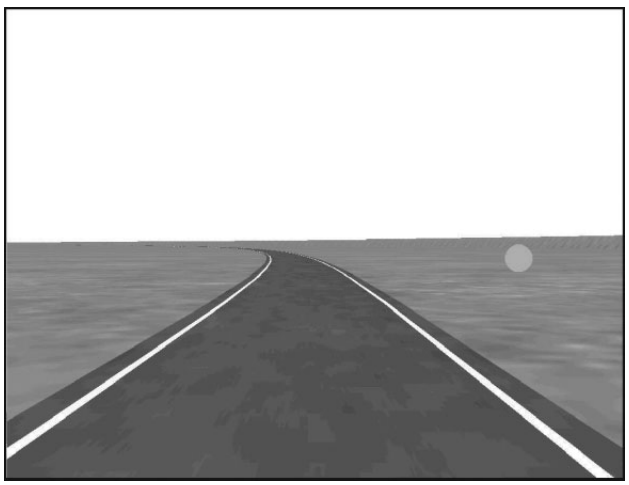

Figure 5. Example of the scene with white light (only middle part of projection, 40 degrees wide) and a target eccentricity of +15 degrees. For each colour condition the whole scene (both target and background) were coloured in the appropriate colour.

important to provide enough optic flow to give the subject a speed sensation while driving (see *Figure 5*). The road scene was presented in white, yellow, red and blue, i.e. there were no hue differences in the scene. This was performed by setting the output channels of the projectors to the above-mentioned RGB values, resulting in four monochrome scenes. It should be noted that (ideally) for each of these colours the *relative* spectral light distribution is the same in the whole image.

Target detection

The subjects responded to the target appearance by pushing a small button that was taped to the right index finger of the subject. Only a tiny tap with the index finger at the steering wheel was needed to activate the button and to record the RT. Eccentricity of target presentation varied randomly. The time between successive target presentations varied randomly between 7 and 11 s (average 9 s). The target was presented for a time period of 3 s and the subject was allowed to react up to 5 s after the start of the target presentation. The target detection performance was determined by measuring the RT and the percentage of missed targets.

Driving behaviour

It is possible that a more demanding driving task has a negative effect on the target detection performance. In order to measure such an effect the subjects were forced to drive at a constant speed (cruise control). It is expected that at a high driving speed the steering task is more difficult than at a low speed. In this experiment we used two speeds, 70 and 100 km h^{-1}. The driving behaviour was measured by recording the position of the car on the road and the turning angle of the steering wheel. This data was used to calculated the following driving behaviour measures:

(1) Standard deviation of lateral position (SDLP) (m).
(2) Percentage of time outside lane (POL) (%). Percentage of the time that the car side was over the left or right line.
(3) Time to line crossing (TLC) (s). Calculated by dividing the distance between the car side and line by the lateral speed (van Winsum *et al*., 2000).
(4) Standard deviation of the steering wheel position (SDS) (radians).
(5) Steering wheel reversal rate (SRR) (1 s^{-1}). The number of steering wheel reversals per unit of time. Reversals were counted when the steering wheel angle changed by more than 2 degrees in the opposite direction.
(6) High frequency area (HFA). The steering wheel position signal in terms of angle in degrees was Fourier transformed. HFA equals the energy content of the high frequencies (0.3–0.6 Hz) divided by the total energy (0–0.6 Hz).

It is assumed that the driving task becomes more difficult when the SDLP and the POL become larger and the TLC becomes shorter. The steering wheel measures are indicators for the steering effort. A higher SDS, SRR, and HFA is an indication for a higher steering effort and a reaction to a more difficult and demanding steering task (Blaauw, 1984).

Subjects

Twenty-one paid subjects participated in the experiment (12 male and nine female) with ages between 20 and 65 (average 21.9, standard deviation = 12.3). All subjects had normal colour vision, tested with the Ishihara test and the Farnsworth Tritan Test (Fletcher and Voke, 1985). They had normal visual acuity. The TNO Landolt-C visual acuity (reciprocal of the minimum-resolvable Landolt-C gap size in min arc) of the subjects varied between 1.25 and 2 (average = 1.81, S.D. = 0.36). Three subjects wore glasses. All subjects had a driving license.

Procedure

Before the experiment the subjects read the instruction sheet. They were told that their first and most important task was to keep the car between the lines as well as possible. It was not necessary to change gears or to use the accelerator or brake pedal, because the driving speed was kept at a constant driving speed by the driving simulator, which acted as an automatic car with the cruise control turned on. In order to ensure a proper dark adaptation the subjects were stationed in the dark experimental room at least 20 min before the experiment.

Each subject drove 28 runs. In each run a different variant of the combination of two speeds, four colours, and four luminance levels was measured (except blue and red for highest light level luminances). During each run the target was presented in a random manner three times at six eccentricities (18 presentations per run). In total the experiment counted 28 runs × 18 presentations × 21 subjects = 10584 target presentations. Each condition was measured 63 times (21 subjects × 3 measurements). Half of the subjects started with the high light conditions (1 and 10 cd m^{-2}) and half of the subjects with the low light conditions (0.1 and 0.01 cd m^{-2}).

One run lasted almost 4 min. The total experiment for one subject lasted about 4 h, with including breaks (after each four or eight runs) and instruction. In order to get used to the driving simulator and the target detection task the subjects did one or two practice runs before the actual experiment.

Results

Target detection

The statistical analysis of the target detection data was performed with an analysis of variance (ANOVA) with speed, luminance, colour and eccentricity as independent variables and RT and missed targets as dependent variables. As it was not possible to reach the highest luminance level of 10 cd m^{-2} for the colours red and blue, the ANOVA was divided in two parts. The first ANOVA was performed for all four colours (white, yellow, red, blue) combined with three luminance levels (0.01, 0.1, 1 cd m^{-2}). In the second ANOVA only the colours white and yellow were considered for all four luminance levels (0.01, 0.1, 1, 10 cd m^{-2}). For all significant effects of the ANOVA we performed a *post hoc* Newman–Keuls test. *Table 4* shows the results of the ANOVA in terms of the probability (p) that the effect is based on chance. There is a significant effect of all dependent variables, except for speed. There are several significant interactions, which will be addressed below. Note that the first ANOVA is the most important one because it covers the majority of the data.

The overall effect of the background luminance on the RT and the percentage of missed targets is plotted in *Figure 6*. Low light levels have an adverse effect on the performance; the RTs are longer and the number of missed targets is larger. For the lowest luminance level of 0.01 cd m^{-2} the RT is almost a factor of two longer than for a photopic level at 10 cd m^{-2}. More than 30% of the targets were missed at scotopic light level; in the photopic region this fell to only about 0.6%. As the luminance level increases the RT and percentage of missed targets decrease and for high luminances at photopic light levels it approaches an asymptotic level.

Table 4. Results of statistical analysis (ANOVA) in terms of *p*-values for the dependent variables reaction time (RT) and missed targets

	p-values			
	RT		Missed targets	
Effect	**ANOVA 1**	**ANOVA 2**	**ANOVA 1**	**ANOVA 2**
Main effects				
Speed	0.6732	0.4112	0.3126	1.0000
Luminance	**0.0000**	**0.0000**	**0.0000**	**0.0000**
Colour	**0.0000**	**0.0000**	**0.0000**	**0.0000**
Eccentricity	**0.0000**	**0.0000**	**0.0000**	**0.0000**
Interactions				
Speed × luminance	0.9806	0.1907	0.4816	0.1561
Speed × colour	0.3946	0.5951	0.3101	0.0710
Luminance × colour	**0.0000**	**0.0000**	**0.0000**	**0.0000**
Speed × eccentricity	**0.0000**	0.1736	0.8396	0.9627
Luminance × eccentricity	**0.0000**	**0.0000**	**0.0000**	**0.0000**
Colour × eccentricity	**0.0000**	0.1622	**0.0000**	0.1125
Speed × luminance × colour	0.6949	0.8431	0.3469	0.1561
Speed × luminance × eccentricity	**0.0000**	**0.0379**	0.8622	0.9531
Speed × colour × eccentricity	**0.0000**	0.5730	0.9472	0.9909
Luminance × colour × eccentricity	**0.0000**	0.1695	**0.0000**	0.0818
1 × 2 × 3 × 4	**0.0000**	0.1073	0.9998	0.9989

The statistically significant interactions ($p < 0.05$) are printed in bold.
ANOVA 1, without luminance of 10 cd m^{-2}; ANOVA 2, without colours red and blue.

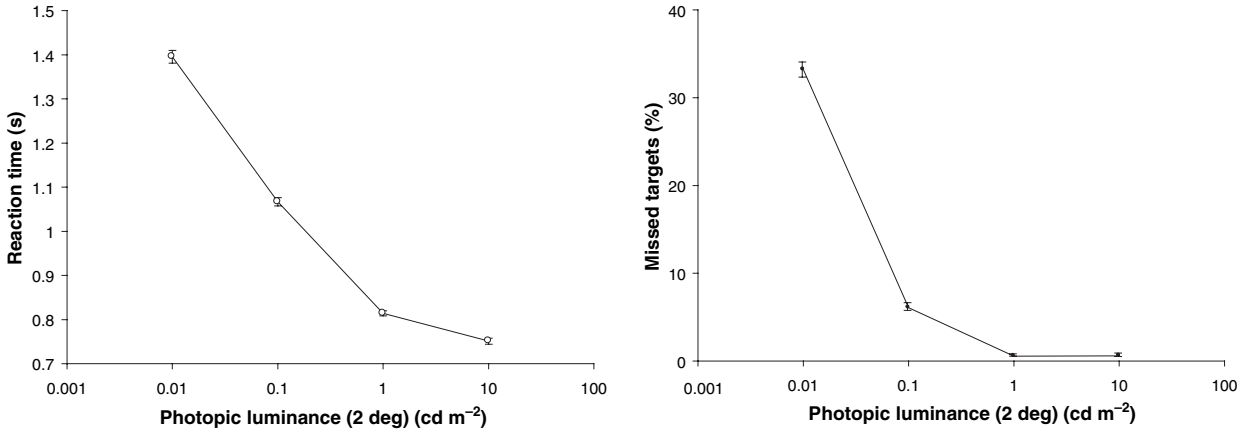

Figure 6. Reaction time (left) and missed targets (right) as a function of the background luminance, averaged over all conditions. The error bars indicate the standard error of the mean.

Figure 7 shows the overall effect of eccentricity on target detection. The longest RTs and the most missed targets were found at large eccentricities of −15 and +15 degrees. There is little difference for eccentricities of 5 and 10 degrees.

For the goal of this study the interactions between the luminance, colour, and eccentricity are of more importance than the main effects. Interaction in this case shows that certain combinations of luminance, colour, eccentricity, and speed values have an additional effect on the target detection performance, i.e. the combination is more than the sum of the separate main effects. For RT there was a three-way interaction between luminance, colour, and eccentricity (and also three possible two-way interactions of these three variables, see *Table 4*). This interaction effect is illustrated in *Figure 8*, where an overview is given of the target detection performance (RT and missed targets) as a function of eccentricity, colour and luminance. As no main effect of speed was found the data was averaged over the two speeds. As seen before in *Figures 6* and *7* the RT increases when the luminance (L) decreases and the eccentricity becomes larger. For the two lowest luminance levels the colour red has the longest RT and the highest percentage of missed targets, particularly for large eccentricities. Differences between colours arise for luminances below 1 cd m^{-2}. The percentage of missed targets shows similar effects. Note that the large percentage of missed

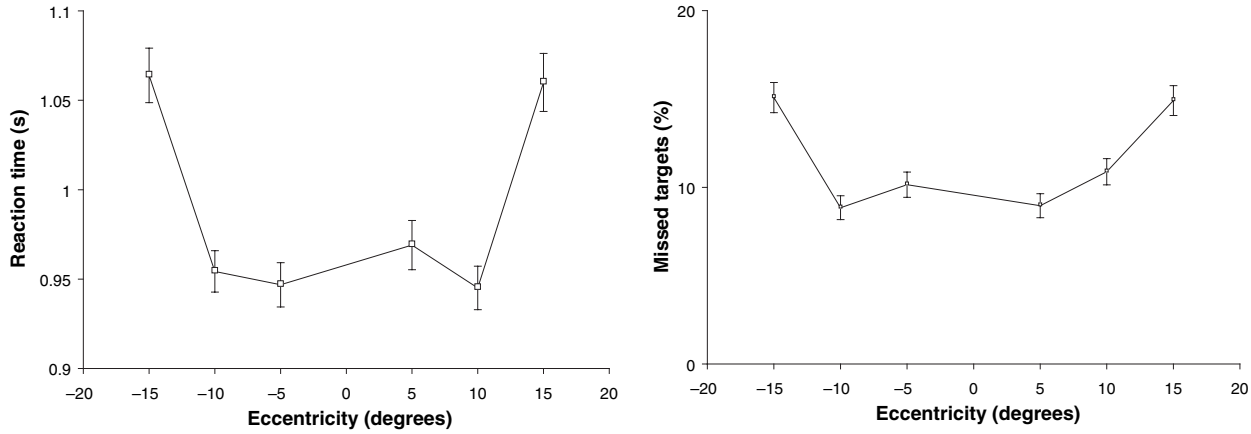

Figure 7. Reaction time (left) and missed targets (right) as a function of eccentricity, averaged over all conditions. The error bars indicate the standard error of the mean.

targets at low luminance levels, in particular for red, is accompanied by a larger spread in the RT data.

No main effect of speed was found. However, we did find a significant four-way interaction between speed, luminance, colour and eccentricity. This interaction is shown graphically in *Figure 9*. There is a difference between a speed of 70 km h^{-1} and a speed of 100 km h^{-1} for the RT as a function of eccentricity for a combination of a low luminance of 0.01 cd m^{-2} and a red colour. For a high speed this function is asymmetrical; the RT for −15 degrees is larger and the RT for +10 degrees is smaller than for a low speed. This effect might be explained as follows. At a high speed the driving task is more difficult than at a low speed. When the steering task is more demanding the subjects have to concentrate more on the middle and the right side of the road (the car was driven on the right hand side of the road), in order to keep the car between the lines. The larger eccentricities on the left are therefore increasingly neglected and the performance is poorer.

Driving behaviour

As the various target eccentricities occurred randomly within one run it was not possible to separate out the driving behaviour effects related to this variable. The driving behaviour measures were averaged over each run. Hence, the eccentricity was omitted in the ANOVA for the driving behaviour and the independent variables were speed, luminance, and colour. The dependent variables were the six driving behaviour measures (SDLP, POL, TLC, SDS, SRR, HFA).

Table 5 shows the results of the ANOVA for the driving behaviour measures. A statistically significant main effect on all driving behaviour measures was found for the variables speed, luminance and colour, except for the effect of colour on HFA.

The most noticeable interaction is luminance × colour, which was found to be significant for four of the six driving behaviour measures. This means that the behaviour measures are dependent on colour, but this dependency varies with luminance level. Furthermore all two-way interactions are statistically significant for TLC and SDS.

The SDLP depends on speed (*Figure 10*). A higher speed results in a slightly larger SDLP. At a high speed and low light level, it is more difficult to drive a smooth course: this is particularly true for the red colour at a high speed, which caused the interaction effects. Differences between all colours were found, except between white and yellow. The POL and TLC measures are not illustrated, but they show almost the same pattern as the SDLP. It should be noted that TLC is small when POL and SDLP are large.

Speed has a large effect on the SDS (*Figure 11*). A higher speed and lower luminance results in larger steering wheel movements. Red gives the highest and blue the lowest SDS values at 0.01 cd m^{-2}. Red differs from all other colours for the lowest luminance. The SRR and HFA measures, which are closely correlated with SDS and therefore show very similar results, are not plotted.

In conclusion, a higher speed and a lower luminance result in more driving errors and a higher steering effort. This is especially the case for the combination of a low luminance and a red colour.

Modelling

The target detection results in this study are presented as RT and percentage missed targets as a function of background light level in terms of photopic luminance. It appears that for the lower luminances the curves for the various colours differ; or in statistical terms, there is

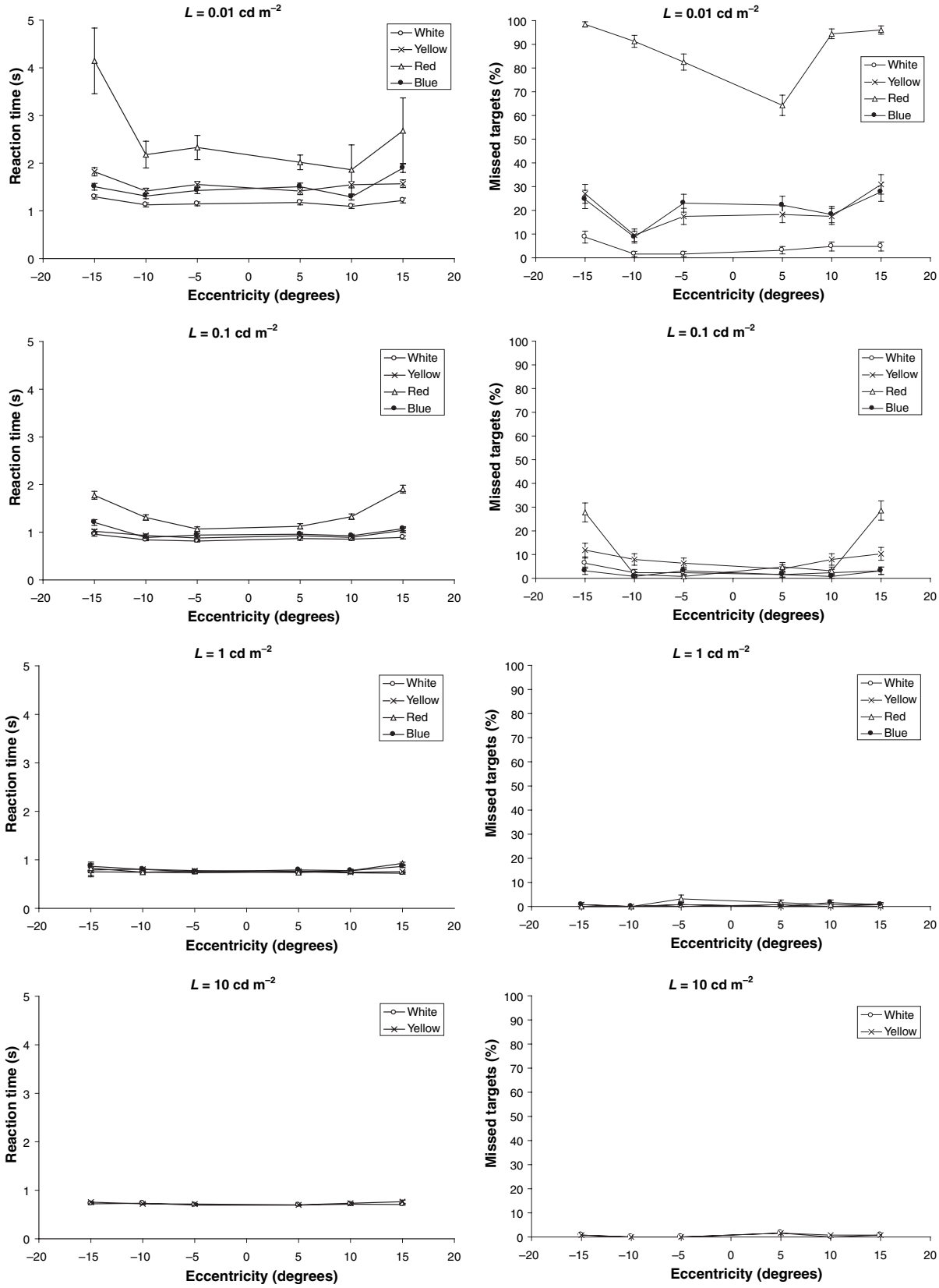

Figure 8. Reaction time (left) and percentage missed targets (right) as a function of eccentricity, colour, and luminance. The error bars indicate S.E. of the mean. L = photopic luminance (2 degree observer).

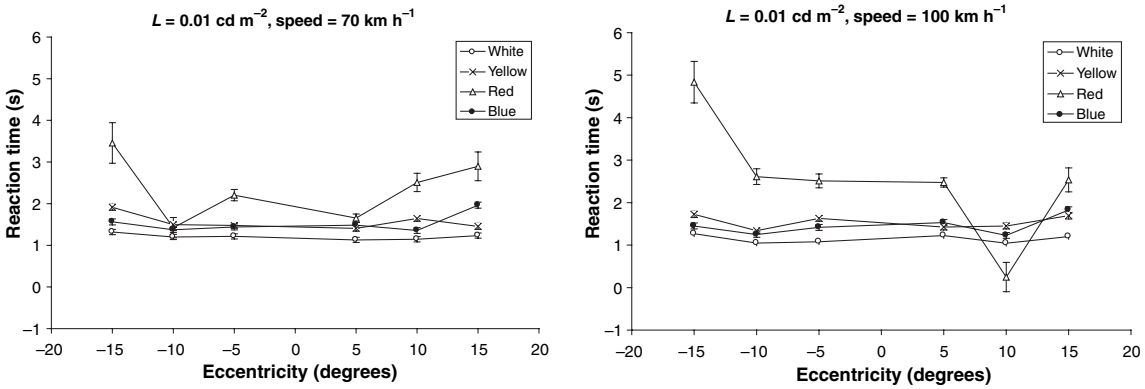

Figure 9. Reaction times as a function of eccentricity and colour at 0.01 cd m^{-2} for 70 km h^{-1} (left) and 100 km h^{-1} (right).

Table 5. Results of statistical analysis (ANOVA without luminance of 10 cd m^{-2}) in terms of *p*-values for the driving behaviour measures (see text for explanation of abbreviation)

	***p*-values**					
Effect	**SDLP**	**POL**	**TLC**	**SDS**	**SRR**	**HFA**
Main effects						
Speed	**0.000**	**0.000**	**0.000**	**0.000**	**0.000**	**0.000**
Luminance	**0.000**	**0.000**	**0.000**	**0.000**	**0.000**	**0.000**
Colour	**0.033**	**0.002**	**0.005**	**0.005**	**0.036**	0.312
Interactions						
Speed × luminance	0.051	0.536	**0.009**	**0.009**	0.415	0.449
Speed × colour	0.308	0.796	**0.020**	**0.020**	0.789	0.561
Luminance × colour	**0.000**	**0.002**	**0.003**	**0.003**	0.461	0.952
Speed × luminance ×colour	**0.019**	0.796	0.131	0.131	0.966	0.397

Statistically significant effects ($p < 0.05$) are printed bold.

an interaction between colour and photopic luminance. This indicates that the low light levels should be appraised with a spectral luminous efficiency function that differs from the spectral luminous efficiency function at high light levels. If the luminance was measured with a suitable mesopic luminance meter these curves should ideally coincide as a single function for the different colours. The question now is: Is it possible to find a suitable mesopic model for the luminance that describes the data better than the current photopic model does? The four existing mesopic models for RT (He 1, He 2, Rea, UnifL; See *Table 1*) were therefore tested using the RT data measured in the current study. The mesopic luminances were calculated, the RT data as a function of the mesopic luminances were fitted with an existing RT model, and the residual variance of the mesopic model was compared with that of the photopic model.

Mesopic luminance

The mesopic luminances according to the four mesopic models were calculated using the spectral radiance of the various backgrounds used in the experiment, four colours combined with four light levels. In the last four columns of *Table 3* the mesopic luminances for these different conditions are shown, next to the common photopic and scotopic luminances. Note that the colour of background and target in the experiment were always

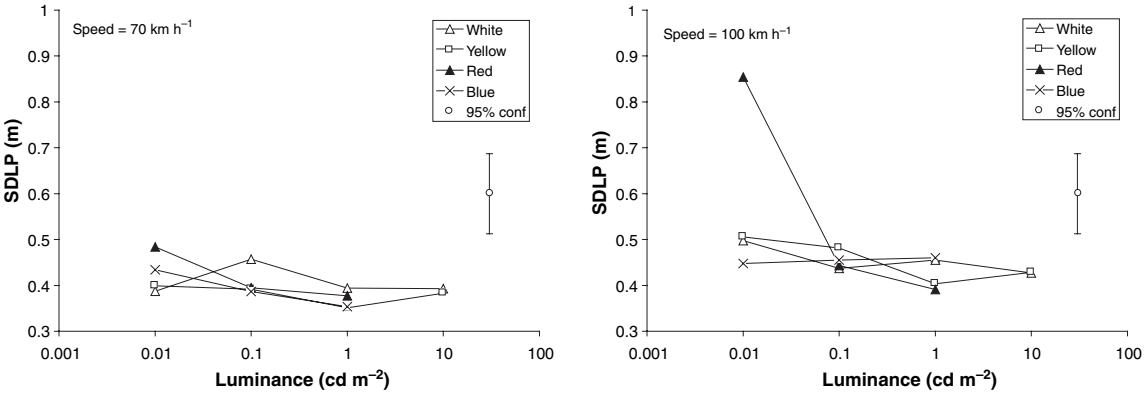

Figure 10. Standard deviation of the lateral position (SDLP) as a function of luminance, colour and speed. The point with error bars indicates the typical 95% confidence intervals for each of the conditions.

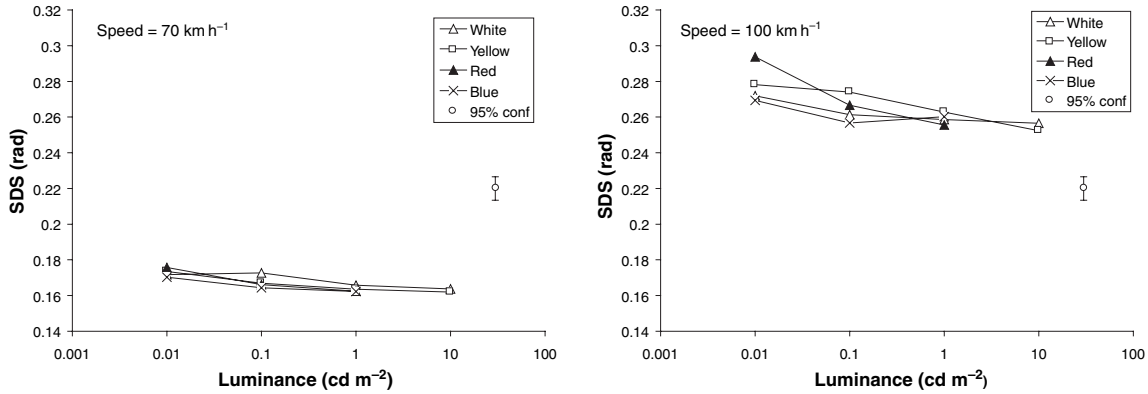

Figure 11. Standard deviation of the steering wheel position (SDS) as a function of luminance, colour and speed. The point with error bars indicates the typical 95% confidence intervals for each of the conditions.

the same, i.e. the relative spectral radiance was always the same for target and background. Therefore the contrast remains the same when applying the various mesopic models to both background and target.

Reaction time model

The RT data as a function of the background luminance level were fitted with the Pieron model (Pieron, 1952; Mansfield, 1973), which can be described by the equation:

$$RT = RT_{\text{inf}} + aL^b \quad (3)$$

RT is the reaction time (s), RT_{inf} is the RT for infinite luminance (s), L is the background luminance (cd m^{-2}), either photopic or mesopic, and a and b are constants. For high luminances the RT approaches a constant value RT_{inf}. For lower luminances the RT increases according to a power function.

The RTs were averaged over subjects, left and right eccentricity, driving speed, and repeated measurements. For each (absolute) eccentricity (5, 10, 15 degrees) the RT model of equation (3) was fitted to these averaged RTs, with the luminance expressed as photopic luminance (CIE 2 degree observer) and four mesopic luminances. A separate fit was determined for each eccentricity with the data of all colours combined in one fit. This is illustrated in *Figure 12*. The left column shows averaged RT data as a function of the photopic luminance (CIE 2 degrees observer) and the right column the mesopic luminance for one of the models (UnifL). The graphs of the other mesopic models are very similar and are therefore not shown. The best fit of the RT model for the data points of all four different colours is obtained when the luminance is expressed in mesopic luminance. Note that for an ideal mesopic model the data point of all colours should coincide perfectly at a single curve of the RT model.

In *Table 6* all parameters of the RT model are listed for the photopic model and the four mesopic models. The exponent b varies between approximately −0.4 and −0.5, which is different from the expected value of −0.31 (Mansfield, 1973). The RT for infinite luminance (RT_{inf}) is more or less constant at a level of about 0.66 s.

The residual variance was used as a quantitative indicator of how well the mesopic model fits to the data. This was determined by calculating the summation of the squares of the differences between measured RT and the RT model, divided by the number of measurements. The residual variance is calculated for each luminance model by summing up the squares of the differences for the three eccentricities and the four colours. *Table 7* shows the results of this statistical analysis. The residual variance is determined for $n = 42$ data points, i.e. 14 luminance-colour combinations (four light levels times four colours minus the two highest light levels for the colours red and blue) times three eccentricities (see *Figure 12*). The number of the degrees of freedom d.f. $= n - 1$, which is 41 for the reference condition with no RT model ($RT = RT_{\text{ave}}$). In case of application of the Pieron RT model the d.f. are less than 9, which is the number of parameters used in Pieron RT model times the number of eccentricities (3×3). The correlation coefficient, r, is a measure for the goodness of the fit; 0 is a bad fit and 1 is a perfect fit. Note that the correlation coefficient is zero for the reference condition, when the function RT = f(luminance) is a horizontal line at the average RT ($RT = RT_{\text{ave}}$). When the RT model of equation (3) is used in combination with the photopic luminance the correlation coefficient is 0.74. Applying a mesopic model gives a slightly higher correlation of about 0.86. The correlation coefficient squared (r^2) indicates the percentage of the total variance that can be explained by the model. An ideal model can explain 100% of the variance. The photopic model explains 55% of the variance, but when a mesopic model is applied this is improved to 75%. The remainder of the variance is probably caused by improper models, measuring errors, and spread in the subject data. The

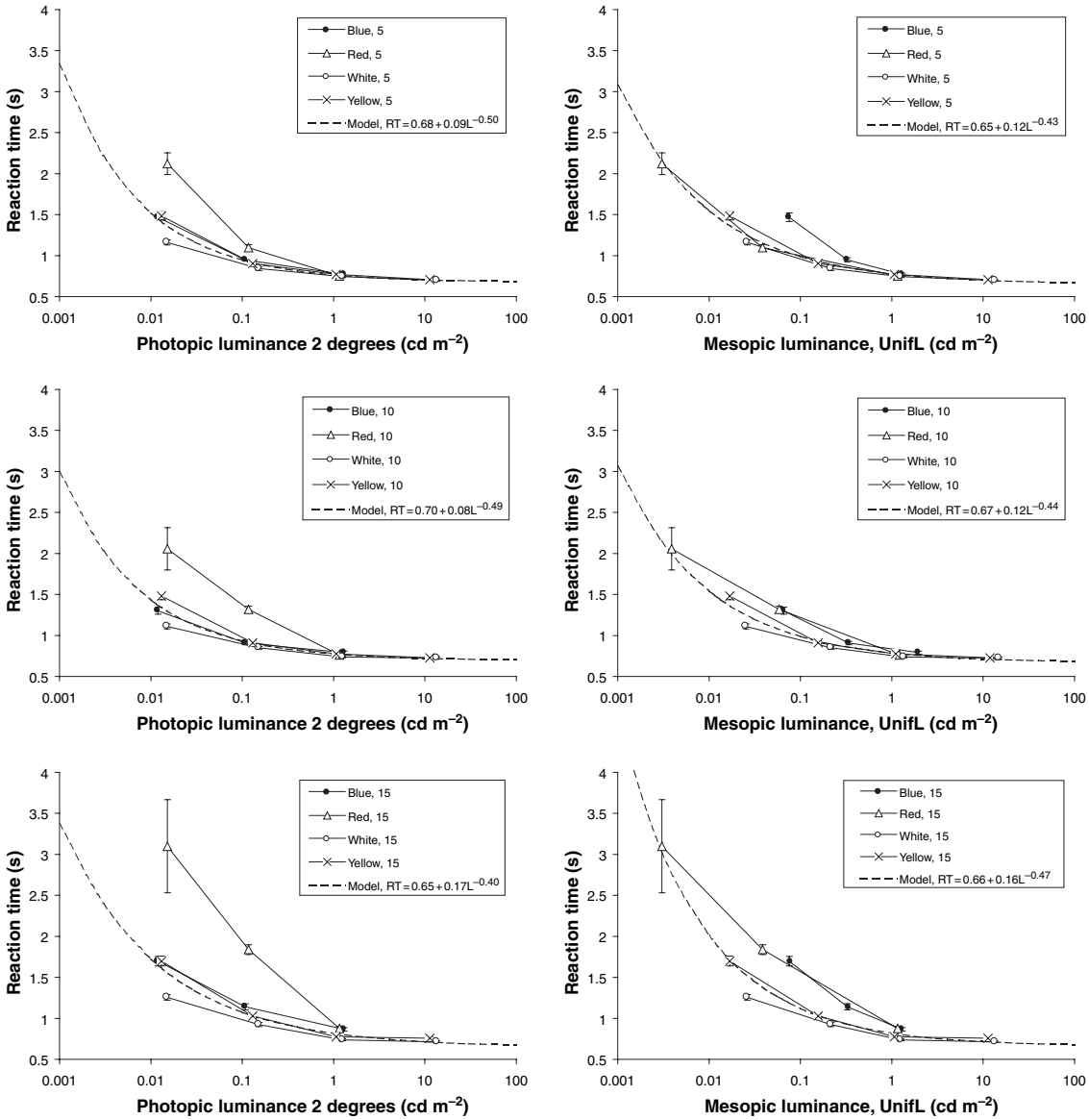

Figure 12. Reaction time as a function of photopic luminance (CIE 2 degree observer, left column) and mesopic luminance (unified luminance model, right column; Rea *et al.*, 2004), for absolute eccentricities of 5 degrees (upper row), 10 degrees (middle row), and 15 degrees (lower row), and four colours. The dashed line is the best fitting model according to equation (3). The error bars indicate the standard error of the mean (SEM).

mesopic models seem to be better than the photopic model for describing the RT data over a large range of light levels and various colours.

The lower part of *Table 7* shows the statistically significant differences (tested with an *F*-test) of the various luminance model combinations. The figures show whether a difference between the two model variances is statistically significant ($p < 0.05$). The most interesting data are the comparisons of the mesopic and photopic models. The Rea and UnifL mesopic models are statistically different ($p = 0.045$, $p = 0.036$) from, and thus better than, the photopic model. The He 1 and He 2 mesopic models are not statistically different from photopic, although the *p*-values approach significance ($p = 0.057$, $p = 0.067$). As there is no significant difference between the mesopic models it is difficult to conclude that the Rea and UnifL models perform better than the He 1 and He 2 models.

Discussion

Comparison with other experiments

In this simulator experiment we found that target detection performance decreases with decreasing background luminance and increasing eccentricity. The target detection performance in particular is poorer for the red colour under these conditions. In general, these

Eccentricity (degrees)	Parameter	Photopic	Mesopic			
			He1	He2	Rea	UnifL
5	*a*	0.086	0.125	0.115	0.114	0.123
	Exponent *b*	–0.496	–0.433	–0.457	–0.459	–0.431
	RT_{inf}	0.677	0.656	0.663	0.661	0.654
10	*a*	0.076	0.117	0.106	0.106	0.117
	Exponent *b*	–0.493	–0.439	–0.466	–0.467	–0.437
	RT_{inf}	0.697	0.672	0.681	0.677	0.669
15	*a*	0.168	0.157	0.147	0.147	0.155
	Exponent *b*	–0.403	–0.469	–0.488	–0.488	–0.470
	RT_{inf}	0.648	0.667	0.674	0.674	0.663

Table 6. Parameters of the Pieron model for the photopic (2 degrees) luminance and four models for mesopic luminance

Luminance model	RT model	*n*	d.f.	Residual variance	*r*-value	r^2-value
–	No ($RT = RT_{ave}$)	42	41	0.1140	0	0
Photopic, $V(\lambda)$	$RT = RT_{inf}+a{\cdot}L^b$	42	32	0.0292	0.744	0.553
Mesopic, He 1	$RT = RT_{inf}+a{\cdot}L^b$	42	32	0.0165	0.855	0.731
Mesopic, He 2	$RT = RT_{inf}+a{\cdot}L^b$	42	32	0.0171	0.850	0.723
Mesopic, Rea	$RT = RT_{inf}+a{\cdot}L^b$	42	32	0.0159	0.861	0.741
Mesopic, UnifL	$RT = RT_{inf}+a{\cdot}L^b$	42	32	0.0153	0.866	0.749

Luminance models	*F*-ratio	d.f. 1	d.f. 2	*p*-value	Significance
No vs photopic	3.91	41	32	**0.000071**	S
He 1 vs photopic	1.77	32	32	0.057	NS
He 2 vs photopic	1.71	32	32	0.067	NS
Rea vs photopic	1.84	32	32	**0.045**	S
UnifL vs photopic	1.91	32	32	**0.036**	S
He 1 vs He 2	1.03	32	32	0.464	NS
He 1 vs Rea	1.04	32	32	0.455	NS
He 1 vs UnifL	1.08	32	32	0.413	NS
He 2 vs Rea	1.08	32	32	0.419	NS
He 2 vs UnifL	1.11	32	32	0.380	NS
Rea vs UnifL	1.04	32	32	0.460	NS

Table 7. Statistical analysis of the fitting RT model when applying different luminance models

Statistically significant differences are indicated by a bold *p*-value.
n, number of data points; *r*, correlation coefficient; r^2, fraction explained variance.

results are in accordance with the findings in other experiments that were performed in a driving context (Bullough and Rea, 2000; Akashi and Rea, 2002; Lingard and Rea, 2002). In these experiments the performance for low light levels and large eccentricities is relatively low when the S/P ratio is low. In our experiment the colour red also has a low S/P ratio of about 0.2, compared with about 2 for white (*Table 3*). However, we did not find a difference between blue and yellow, which have quite different S/P ratios of 1.4 and 9. Probably the spread in the data collected in our simulator experiment was too large to reveal a statistically significant difference between these two colours.

Eccentricity

In the current experiment no difference was found in performance between the eccentricities of 5 and 10 degrees, when the data was averaged over all conditions (*Figure 7*). Apparently it was not more difficult to detect the target at 10 degrees than it was at 5 degrees. One of the possible reasons could be eye movements of the subjects. The subjects were instructed to keep the car between the lines of the road. For this they had to keep their eyes for a certain part of the time at the road ahead. However, they were allowed to look at other parts of the scene. The eyes fixating other than straight ahead probably causes the levelling effect with regard to eccentricity. Unfortunately it is not possible to compare the results with an eccentricity of zero degrees, where the target should be detected most easily and certainly the shortest RT would be measured. Because of the limitations of the method, i.e. a simulated road right ahead, the target was not presented at zero eccentricity.

Modelling mesopic

The data of the current experiment were modelled with four mesopic models based on RT measurements at eccentricities between 12 and 15 degrees. The

eccentricities of the current experiment ranged from 5 to 15 degrees, which is somewhat wider. It is possible that the mesopic models do not predict the data very well for the smallest eccentricities. At least for an eccentricity of zero degrees, i.e. foveal vision, it is expected that even at low light levels the spectral luminous efficiency function for photopic vision, $V(\lambda)$, is still valid (He *et al.*, 1997) rather than the spectral luminous efficiency function for scotopic vision, $V'(\lambda)$, as applied in the current models for the off-axis conditions. A mesopic model that has the eccentricity as an input parameter and can therefore discriminate between eccentricities is more suitable. The ideal mesopic model should fit with the current standard spectral efficiency functions and should be able to predict the mesopic luminances at all eccentricities between 0 and say 20 degrees in a continuous way, for all light levels. For foveal vision (on-axis) the $V(\lambda)$ can be applied for any light level. For peripheral vision at photopic light levels the $V_{10}(\lambda)$ spectral efficiency function might be more appropriate than $V(\lambda)$. Only at low light levels and for off-axis targets should the spectral luminous efficiency function for scotopic vision, $V'(\lambda)$, be applied. For all intermediate conditions a proper function must be developed for the weighting between $V(\lambda)$, $V_{10}(\lambda)$, and $V'(\lambda)$. To do this properly more reliable experimental data are needed.

Conclusions

A target detection experiment was performed during a driving task in a driving simulator at mesopic light levels. For target eccentricities between 5, 10 and 15 degrees we found that target detection performance (RT and missed targets) decreases with decreasing background luminance and increasing eccentricity. The performance for red is worse than for other colours at low luminances. These measured data are consistent with similar experiments in the laboratory, with a few deviations, which can be labelled as typical for the driving situation.

A higher driving speed and lower luminance result in more driving errors and a higher steering effort. This is especially so for the combination of a low luminance and a red colour. The data suggest that in this condition the subjects tend to look more in the right middle of the scene and neglect left off-axis targets. Simple models for mesopic luminance, based on RT, describe the data better than the photopic model, which is currently widely used in photometry.

Acknowledgements

This study was supported by the European Commission, Project MOVE (Mesopic Optimisation of Visual Efficiency), Fifth Framework programme (G6RD-CT-2001-00598).

References

Akashi, Y. and Rea, M. (2002) Peripheral detection while driving under a mesopic light level. *J. Illum. Eng. Soc.* **31,** 85–94.

Ashizawa, S., Ikeda, M. and Nakano, Y. (1985) Experiments and analysis on the brightness of colored clothes at various illumination levels. *J. Illum. Eng. Inst. Jpn.* **69,** 274–280.

Blaauw, G. J. (1984) Car driving as a supervisory control task. (Thesis), TNO Human Factors, Soesterberg, The Netherlands.

Bullough, J. D. and Rea, M. S. (2000) Simulated driving performance and peripheral detection at mesopic and low photopic light levels. *Lighting Res. Technol.* **32,** 194–198.

CIE (1978) *Light as a True Visual Quantity: Principles of Measurement*. CIE Publication No. 41/Reprint 1994. Central Bureau of the Commission Internationale de l'Eclairage, Vienna.

CIE (1983) *The Basis of Physical Photometry*. CIE Publication No. 18.2. Central Bureau of the Commission Internationale de l'Eclairage, Vienna.

CIE (1986) *Colorimetry*. CIE Publication No. 15.2. Central Bureau of the Commission Internationale de l'Eclairage, Vienna.

CIE (1989) *Mesopic Photometry: History, Special Problems and Practical Solutions*. CIE Publication No. 81. Central Bureau of the Commission Internationale de l'Eclairage, Vienna.

CIE (2001) *Testing of Supplementary Systems of Photometry*. CIE Publication No. 141. Central Bureau of the Commission Internationale de l'Eclairage, Vienna.

De Clercq, G. (1985) Fifteen years of road lighting in Belgium. *Int. Lighting Rev.* **1,** 2–7.

Eloholma, M. and Halonen, L. (2003) New approach for the development of mesopic dimension scales. In: *Proceedings of the CIE Symposium 2002 on Temporal and Spatial Aspects of Light and Colour Perception and Measurement* (ed. Schanda J.), Veszprém, Hungary, August 22 and 23. Publication CIE x025:2003, CIE, Vienna, Austria, pp. 61–64.

Eloholma, M., Viikari, M., Halonen, L., Walkey, H., Goodman, T., Alferdinck, J., Frieding, A., Schanda, J., Bodrogi, P. and Várady, G. (2005) Mesopic models – from brightness matching to visual performance of night-time driving: a review. *Lighting Res. Technol.* **37,** 155–175.

Fletcher, R. and Voke, J. (1985) *Defective Colour Vision*. Adam Hilger Ltd, Bristol, UK.

He, Y., Rea, M., Bierman, A. and Bullough, J. (1997) Evaluating light source efficacy under mesopic conditions using RTs. *J. Illum. Eng. Soc.* **26,** 125–138.

He, Y., Bierman, A. and Rea, M. S. (1998) A system of mesopic photometry. *Lighting Res. Technol.* **30,** 175–181.

Ikeda, M. and Shimozono, H. (1981) Mesopic luminous-efficiency functions. *J. Opt. Soc. Am.* **71,** 280–284.

Kaptein, N. A., Hogema, J. H. and Folles, E. (1997) Dynamic Public Light (DYNO). In: *Proceedings Lux Europa*, 1997, (eds. Burghout F. *et al.*), pp. 461–467.

Kinney, J. A. S. (1958) Comparison of scotopic, mesopic, and photopic spectral sensitivity curves. *J. Opt. Soc. Am.* **48,** 185–190.

Kokoschka, S. (1980) Photometrie niedriger Leuchtdichten durch eine äquivalente Leuchtdichte des 10° -Feldes. *Licht-Forschung* **1,** 3–15.

Kokoschka, S. and Bodmann, H. W. (1975) Ein konsistentes System zur photometrischen Stralungsbewertung im gesamten Adaptationsbereich. In: *Proceedings of the 18th Session of the CIE* (ed. Lompe A.), Commission Internationale de l'Eclairage, Vienna, Austria, pp. 217–225.

Lewin, I. (2001) Lumen effectiveness multipliers for outdoor lighting design. *J. Illum. Eng. Soc.* **30,** 40–52.

Lewis, A. L. (1998) Equating light sources for visual performance at low luminances. *J. Illum. Eng. Soc.* **27,** 80–84.

Lewis, A. L. (1999) Visual performance as a function of spectral power distribution of light sources at luminances used for general outdoor lighting. *J. Illum. Eng. Soc.* **28,** 37–42.

Lingard, R. and Rea, M. (2002) Off-axis detection at mesopic light levels in a driving context. *J. Illum. Eng. Soc.* **31,** 33–39.

Mansfield, R. J. W. (1973) Latency functions in human vision. *Vision. Res.* **13,** 2219–2234.

Owens, D. A. and Sivak, M. (1993) *The Role of Reduced Visibility in Nighttime Road Fatalities* (Report UMTRI-93-33). The University of Michigan Transportation Research Institute, Ann Arbor, Michigan, USA.

Palmer, D. A. (1968) Standard observer for large-field photometry at any level. *J. Opt. Soc. Am.* **58,** 1296–1299.

Pieron, H. (1952) *The Sensations: Their Functions, Processes and Mechanisms*. (Translated by M.H. Pirenne and B.C. Abbott). Frederick Muller Ltd, London.

Rea, M. S. (2001) The road not taken. *Lighting J.* **66,** 18–25.

Rea, M. S., Bullough, J. D., Freyssinier Nova, J. P. and Bierman, A. (2003) X (A system of mesopic photometry based on RT measurement). In: *Proceedings of the CIE Symposium 2002 on Temporal and Spatial Aspects of Light and Colour Perception and Measurement* (ed. Schanda J), Veszprém, Hungary, August 22 and 23. Publication CIE x025:2003, CIE, Vienna, Austria, pp. 51–58.

Rea, M. S., Bullough, J. D., Freyssinier Nova, J. P. and Bierman, A. (2004) A proposed unified system of photometry. *Lighting Res. Technol.* **36,** 85–111.

Rumar, K. (2002) Night driving accident in an international perspective. In: *Proceedings of the First International Congress* "Vehicle and Infrastructure Safety Improvement in Adverse Conditions and Night Driving" VISION (ed. Charlet M.), Rouen, September 24 and 25, Société des Ingénieurs de l'Automobile SIA, Suresnes, France.

Sagawa, K. and Takeichi, K. (1986) Spectral luminous efficiency functions in the mesopic range. *J. Opt. Soc. Am. A* **3,** 71–75.

Sagawa, K. and Takeichi, K. (1987) Mesopic photometry system based on brightness perception. In: *Proceedings of the 21st Session of the CIE* (ed. Aldworth R. C.), Venice, 17–25 June, International Commission on Illumination (CIE), Vienna, pp. 34–37.

Sagawa, K. and Takeichi, K. (1992) System of photometry for evaluating lights in terms of comparative brightness relationships. *J. Opt. Soc. Am. A* **9,** 1240–1246.

Trezona, P. W. (1987) A system of general photometry designed to avoid assumptions. In: *Proceedings of the 21st Session of the CIE* (ed. Aldworth R. C.), Venice, 17–25 June, International Commission on Illumination (CIE), Vienna, pp. 30–33.

Trezona, P. W. (1990) Software for a system of photometry including the mesopic region. *Die Farbe* **37,** 221–230.

Vis, A. A. (1994) *Street Lighting and Road Safety on Motorways (Report D-94-18, Paper Presented at the International Conference* "Road Safety in Europe and Strategic Highway Research Program", Lille, France, 26–28 September 1994). SWOV, Institute for Road Safety Research, The Netherlands.

Walters, H. V. and Wright, W. D. (1943) The spectral sensitivity of the fovea and the extrafovea in the Purkinje range. *Proc. R. Soc. Lond. B Biol. Sci.* **131,** 340.

van Winsum, W., Brookhuis, K. A. and de Waard, D. (2000) A comparison of different ways to approximate time-to-line crossing (TLC) during car driving. *Accid. Anal. Prev.* **32,** 47–56.

Wyszecki, G. and Stiles, W. S. (1982) *Color Science: Concepts and Methods, Quantitative Data and Formulae*, 2nd edn. John Wiley & Sons, New York.

Yaguchi, H. and Ikeda, M. (1984) Mesopic luminous-efficiency functions for various adapting levels. *J. Opt. Soc. Am. A* **1,** 120–123.